[d]the Department of Pediatrics, King Abdulaziz Medical City, Jeddah, Saudi Arabia; [e]the Department of Medicine, University of Cambridge, Cambridge, United Kingdom; and [f]the Molecular Immunology Unit, Institute of Child Health, University College London, London, United Kingdom. E-mail: siobhan.burns@ucl.ac.uk. Or: sn262@cam.ac.uk.

*These authors contributed equally to this work.

This work was supported by the Higher Education Funding Council for England (to S.O.B.), The Wellcome Trust (grant no. 095198/Z/10/Z to S.N. and grant no. 090233/Z/09/Z to A.J.T.), The European Research Council (Starting grant 260477 to S.N.), the European Union (FP7 collaborative grant 261441 PEVNET project to S.N.), the National Institute for Health Research Cambridge Biomedical Research Centre (to S.N. and R.D.), Great Ormond Street Hospital Children's Charity (to H.B.G. and F.H.), the National Institute for Health Research Great Ormond Street Hospital Biomedical Research Centre (to K.C.G.), and the National Institute for Health Research University College London Hospitals Biomedical Research Centre (to S.O.B.).

Disclosure of potential conflict of interest: S. O. Burns has received research support from the Higher Education Funding Council for England and the National Institute for Health Research University College London Hospitals Biomedical Research Centre. A. M. Jones has received an honorarium from CSL-Behring for a lecture on subcutaneous immunoglobulin therapy and has received travel support from CSL-Behring for the 2013 AAAAI meeting. S. Nejentsev has received research support from the Wellcome Trust, the European Research Council, and the National Institute for Health Research. The rest of the authors declare that they have no relevant conflicts of interest.

REFERENCES

1. Oeckinghaus A, Hayden MS, Ghosh S. Crosstalk in NF-kappaB signaling pathways. Nat Immunol 2011;12:695-708.
2. Doffinger R, Smahi A, Bessia C, Geissmann F, Feinberg J, Durandy A, et al. X-linked anhidrotic ectodermal dysplasia with immunodeficiency is caused by impaired NF-kappaB signaling. Nat Genet 2001;27:277-85.
3. Filipe-Santos O, Bustamante J, Haverkamp MH, Vinolo E, Ku CL, Puel A, et al. X-linked susceptibility to mycobacteria is caused by mutations in NEMO impairing CD40-dependent IL-12 production. J Exp Med 2006;203:1745-59.
4. Courtois G, Smahi A, Reichenbach J, Doffinger R, Cancrini C, Bonnet M, et al. A hypermorphic IkappaBalpha mutation is associated with autosomal dominant anhidrotic ectodermal dysplasia and T cell immunodeficiency. J Clin Invest 2003;112:1108-15.
5. Picard C, Casanova JL, Puel A. Infectious diseases in patients with IRAK-4, MyD88, NEMO, or IkappaBalpha deficiency. Clin Microbiol Rev 2011;24:490-7.
6. Lahtela J, Nousiainen HO, Stefanovic V, Tallila J, Viskari H, Karikoski R, et al. Mutant CHUK and severe fetal encasement malformation. N Engl J Med 2010;363:1631-7.
7. Alangari AA, Al-Zamil F, Al-Mazrou A, Al-Muhsen S, Boisson-Dupuis S, Awadallah S, et al. Treatment of disseminated mycobacterial infection with high-dose IFN-gamma in a patient with IL-12Rbeta1 deficiency. Clin Dev Immunol 2011;2011:691956.
8. Pannicke U, Baumann B, Fuchs S, Rensing-Ehl K, Holzmann K, Henneke P, et al. A novel SCID due to an IKBKB defect. J Clin Immunol 2012;32:S381-2.
9. Li Q, Van AD, Mercurio F, Lee KF, Verma IM. Severe liver degeneration in mice lacking the IkappaB kinase 2 gene. Science 1999;284:321-5.
10. Tanaka M, Fuentes ME, Yamaguchi K, Durnin MH, Dalrymple SA, Hardy KL, et al. Embryonic lethality, liver degeneration, and impaired NF-kappa B activation in IKK-beta-deficient mice. Immunity 1999;10:421-9.
11. Li ZW, Chu W, Hu Y, Delhase M, Deerinck T, Ellisman M, et al. The IKKbeta subunit of IkappaB kinase (IKK) is essential for nuclear factor kappaB activation and prevention of apoptosis. J Exp Med 1999;189:1839-45.
12. Woronicz JD, Gao X, Cao Z, Rothe M, Goeddel DV. IkappaB kinase-beta: NF-kappaB activation and complex formation with IkappaB kinase-alpha and NIK. Science 1997;278:866-9.
13. Samaniego S, Marcu KB. IKKbeta in myeloid cells controls the host response to lethal and sublethal Francisella tularensis LVS infection. PLoS One 2013;8:e54124.
14. Pasparakis M, Courtois G, Hafner M, Schmidt-Supprian M, Nenci A, Toksoy A, et al. TNF-mediated inflammatory skin disease in mice with epidermis-specific deletion of IKK2. Nature 2002;417:861-6.
15. Pasparakis M. Role of NF-kappaB in epithelial biology. Immunol Rev 2012;246:346-58.

Available online March 27, 2014.
http://dx.doi.org/10.1016/j.jaci.2013.12.1093

A case of partial dedicator of cytokinesis 8 deficiency with altered effector phenotype and impaired CD8$^+$ and natural killer cell cytotoxicity

To the Editor:

Hyper-IgE syndrome (HIES) is a primary immunodeficiency characterized by recurrent infections predominantly involving the skin and lungs, chronic eczema, high serum IgE levels, and eosinophilia. HIES has diverse modes of inheritance. Autosomal-dominant HIES (Mendelian Inheritance in Man [MIM] no. 147060) is caused by mutations in the signal transducer and activator of transcription 3 gene. Most cases of autosomal-recessive HIES are caused by mutations in the gene encoding the dedicator of cytokinesis 8 (DOCK8) (MIM no. 243700). DOCK8 deficiency is characterized clinically by recurrent viral, fungal, and sinopulmonary infections.[1-4] These patients also have severe atopic dermatitis, allergies, and an increased likelihood of developing cancer. DOCK8 deficiency affects both innate and adaptive immunity and causes combined immunodeficiency.

We present a patient who fulfilled clinical and immunological parameters for HIES (see the Case report section in this article's Online Repository at www.jacionline.org). Mutations in the signal transducer and activator of transcription 3 gene were ruled out. At this stage, a DOCK8 deficiency was suspected. Using comparative genome hybridization, a heterozygous deletion of exons 2 to 8 was identified in the *DOCK8* gene (see Fig E1, *A*, in this article's Online Repository at www.jacionline.org). Sequence analysis also demonstrated a heterozygous G > A mutation at position +5 in the 5′ splice donor site of intron 17 (IVS17+5 G>A) deleting the exon 17 (Genbank KC736820). This alteration corresponded to a deletion in the conserved DHR1 domain of the protein (Fig E1, *B* and *C*) and was absent in 50 healthy donors. Some normal *DOCK8* transcripts were present, indicating that the exon 17 splicing mutation did not abrogate normal processing of this allele (Fig E1, *D*). *DOCK8* transcript expression was lower in the patient than in controls in PBMCs, as well as CD4$^+$ and natural killer (NK) cells (Fig E1, *E*); however, the DOCK8 protein was clearly detected in the patient by Western blot, albeit at reduced levels. On the basis of these findings, we conclude that this is a new case of partial DOCK8 deficiency (Fig E1, *F*).

Abnormalities in the T-cell compartment have been described in classical DOCK8 deficiency,[2-4] and we decided to assess the impact of a partial DOCK8 deficiency on T-cell phenotype and function. Our patient showed defective thymopoiesis with an absence of T-cell receptor rearrangement excision circles, reduced recent thymic emigrants, a restricted T-cell repertoire, and decreased naive CD4$^+$ T cells in PBMCs (Table I; see Fig E2, *A*, *B*, and *C*, and Fig E3, *A*, in this article's Online Repository at www.jacionline.org). Furthermore, there was an increase in plasma levels of IL-7 (Table I), which could reflect a compensatory attempt to boost the expansion of recent thymic emigrants cells to overcome the depletion of peripheral CD4$^+$ T cells. Interestingly, in spite of naive CD4$^+$ T-cell lymphopenia, the patient's T-cell proliferation was unaffected and similar to that in controls (Fig E3, *B*). This could be related to the nonexhausted phenotype showed by the patient, with normal levels of T-effector memory CD45RA (TEMRA) CD8$^+$ T cells (Fig E3, *A*), in contrast to classical loss-of-function/expression of DOCK8 in patients

TABLE I. Immunologic features of the patient

Parameter	Normal range	Patient
Lymphocyte count (no./μL) and phenotype (%)	1200-3000	888*
T cells		
$CD3^+$ (/μL)	850-2250	603*
$CD4^+$ (/μL)	500-1450	375*
$CD4^+CD45RA^+CCR7^+$ (naive) (%)	25-72	15*
$CD4^+CD45RA^-CCR7^{+/-}$ (memory) (%)	28-68	82*
$CD8^+$ (/μL)	160-950	208
$CD8^+CD45RA^+CCR7^+$ (naive) (%)	28-61	35
$CD8^+CD45RA^-CCR7^+$ (central memory) (%)	1-10	19*
$CD8^+CD45RA^-CCR7^-$ (effector memory) (%)	5-36	23
$CD8^+CD45RA^+CCR7^-$ (TEMRA) (%)	15-45	18
Activated T cells		
$CD3^+HLA\text{-}DR^+$ (%)	0-10	14*
$CD4^+CD45RO^+HLA\text{-}DR^+$ (%)	3-10	19*
$CD8^+CD45RO^+HLA\text{-}DR^+$ (%)	5-14	6
NK cells		
$CD3^-CD56^+$ (/μL)	60-500	54*
iNKT Cells $CD3^+CD56^+V\beta11^+V\alpha24$ (%)	0.01-1.80	0.0*
B cells		
$CD19^+$ (/μL)	100-500	194
$CD19^+CD27^+$ (%)	12-35	8*
$CD19^+IgD^+CD27^-$ (naive) (%)	57-84	88*
$CD19^+IgD^+CD27^+$ (marginal) (%)	4-12	3*
$CD19^+IgD^-CD27^+$ (switched) (%)	7-25	5*
T-cell proliferation (cpm)		
PHA	>50,000	102,864
Anti-CD3	>9,000	30,212
Anti-CD3+Anti-CD28	>80,000	151,548
Serum immunoglobulins		
IgG† (mg/dL)	700-1600	1130
IgA (mg/dL)	70-400	490*
IgM (mg/dL)	40-230	11*
IgE (IU/mL)	5-165	86
Specific antibodies		
IgG vs *Haemophilus* (mg/dL)	>4× prevalue	Absent*
IgG vs *Pneumococcus* (mg/dL)	>5.40	2.93*
IgG2 vs *Pneumococcus* (mg/dL)	>2.14	2.0*
IgG vs tetanus toxoid (IU/mL)	>0.15	2.1
Serum IL-7 (pg/mL)	0.66-9.24	26*
TRECs (/ug DNA)	3806	<40*
IL-17‡ (pg/mL)	200-700	413
Eosinophils (×1000 μL)	0.0-0.5	0.2

IGIV, Intravenous immunoglobulin; *TREC*, T-cell receptor rearrangement excision circle.
*Altered values in the patient.
†IVIG replacement therapy.
‡IL-17 levels in supernatants from PBMCs cultured 5 d with anti-CD3+anti-CD28.

presenting an exhausted phenotype with high levels of TEMRA $CD8^+$ T cells impairing lymphocyte proliferation. The exhausted phenotype could be associated with replicative senescence resulting from continuous antigen stimulation as seen in repeated viral infections.[4]

$CD8^+$ T-cell subsets were further assessed for the expression of several molecules that change during differentiation from naive to effector cells.[5,6] The patient's $CD8^+$ T cells showed dysregulated expression of some of these markers. CD28, CD127, and CD27 expression on TEMRA $CD8^+$ T cells was higher than that seen in normal controls ($P < .01$). In contrast, these molecules were expressed at lower levels in classical DOCK8 patients than in normal controls[4] (Fig 1, *A*). Furthermore, the percentage of cells expressing CD57 and cytoplasmic perforin in $CD8^+$ and in TEMRA $CD8^+$ T-cells subset was much lower than in other classical DOCK8 patients[4] and even lower than that in controls ($P < .05$) (Fig 1, *B* and *C*). That is, our patient's TEMRA $CD8^+$ T cells showed an abnormal effector phenotype. In addition, the levels of antiviral cytokines (IFN-γ and TNF-α) produced by his PBMCs were also comparable with those of controls (data not shown). The increase in activated memory $CD4^+$ T cells in the patient (Table I) suggested that these cells could be more sensitive to activation-induced cell death. In fact, his $CD4^+$ and $CD8^+$ T cells were more sensitive to Fas-induced apoptosis. Concomitant stimulation with PHA also induced more cell death (see Fig E4, *A*, in this article's Online Repository at www.jacionline.org). Interestingly, the patient's CD95 expression in both $CD4^+$ and $CD8^+$ T cells was higher than levels seen in the controls (Fig E4, *B*). The differences in CD95 expression mainly affected naive $CD4^+$ and $CD8^+$ T cells (mean ± SD, 42.8 ± 14.1 vs 10.2 ± 5.1 in controls, $P = .03$, and 48.9 ± 23.5 vs 5.8 ± 5.6 in controls, $P = .02$, respectively) (Fig E4, *C*). These differences were much greater for all markers tested after anti-CD3 stimulation (Fig E4, *B*). The higher apoptosis and elevated expression of activated markers could reflect a phenotype with sustained activation, in which naive cells also exhibit features of early activation. Functionally, the degranulation of the patient's $CD8^+$ T cells using R69 target cells and anti-CD3 mAb was lower with respect to controls, but these differences were not statistically significant. In addition, patient's $CD8^+$ T cells were significantly less effective at killing R69 target cells than those from controls contrasting with the intact cytotoxicity in classical DOCK8 patients[3] (Fig 1, *D*).

NK cells from DOCK8 patients did not polarize their lytic machinery because of impaired synaptic F-actin accumulation at the NK cell synapse, which is essential for cytotoxicity.[7] In this case, NK lymphocytes have been gradually declining over the life of the patient (data not shown). Furthermore, there is an imbalance between $CD56dimCD16^{+/-}CD3^-$ (cytotoxic function) and $CD56bright\ CD16^{+/-}CD3^-$ (regulatory function) in the patient's NK subsets compared with controls (see Fig E5, *A*, in this article's Online Repository at www.jacionline.org). We also performed phenotypic characterization of NK cells, and, specifically, surface CD16 and cytoplasmic perforin expression were significantly lower in his NK cells than in those of controls (see Table E1 in this article's Online Repository at www.jacionline.org; also see Fig E5, *B*). Overall, stimulation of NK cells with K562 cells resulted in NK-cell activation characterized by the upregulation of CD16, CD25, and CD69. The patient's NK cells showed lower mean fluorescence intensity for CD16 and CD69 than did controls' NK cells (Fig E5, *B*). Furthermore, his NK degranulation and cytotoxicity were significantly lower than in controls (Fig E5, *C* and *D*), in agreement with a recent report.[7]

In summary, we describe a new case of partial DOCK8 deficiency that presents a nonexhausted phenotype of $CD8^+$ T cells likely due to a milder clinical phenotype without life-threatening infections. The altered effector phenotype and impaired CD8 and NK cytotoxicity in this patient are probably related to the essential role of DOCK8 in the regulation of actin dynamics and formation of the immunological synapse, which is required for T-cell activation and acquisition of

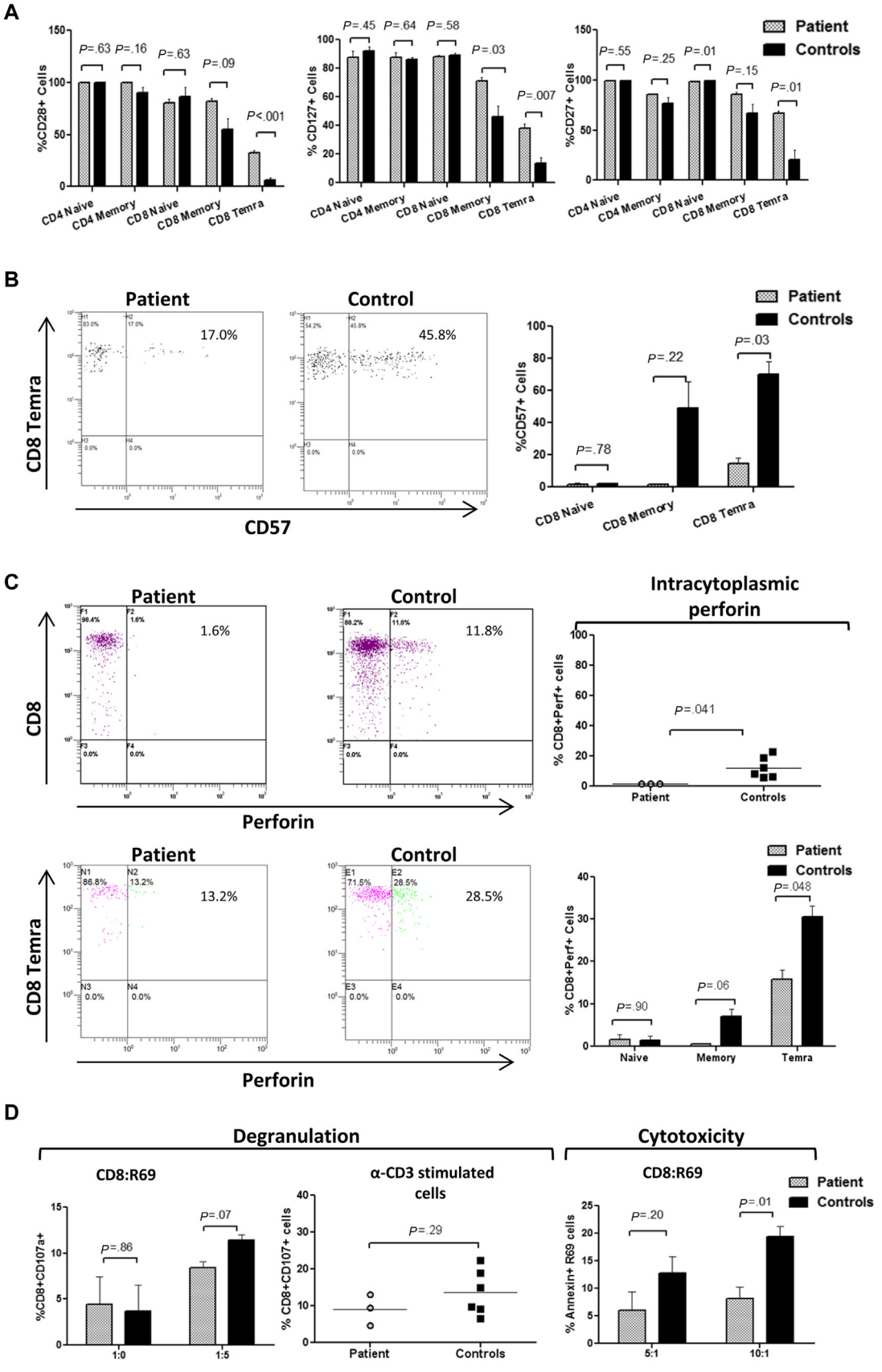

FIG 1. $CD4^+$ and $CD8^+$ phenotype and functional assays. **A,** Expression of CD28, CD127, and CD27 molecules on $CD4^+$ and $CD8^+$ T-cell subsets (mean ± SD of 2 independent experiments). **B** and **C,** *Dot plots*

effector functions.[7,8] In contrast, there are other DOCK8 deficiencies defined as profound combined immunodeficiency by the classical loss-of-function/expression of DOCK8 that present an exhausted T-cell phenotype with increased susceptibility to viral infections and a compromised immunosurveillance. Overall, it would be advisable to study DOCK8 patients in depth characterizing the protein expression, phenotype, and immune functions to be able to establish genotype-phenotype correlations.

We thank Professor José Ramón Regueiro for critical reading of the article, Maite Fernández for her care of the patient, and Miguela Menchén and María José Díaz-Madroñero for their technical assistance.

Raquel Ruiz-García, BS[a]
Sara Lermo-Rojo, BS[a]
Luis Martínez-Lostao, MD, PhD[b]
Esther Mancebo, PhD[a,c]
Sergio Mora-Díaz, BS[a]
Estela Paz-Artal, MD, PhD[a,c]
Jesús Ruiz-Contreras, MD, PhD[c,d]
Alberto Anel, PhD[b]
Luis I. González-Granado, MD[c,d]
Luis M. Allende, PhD[a,c]

From [a]Servicio de Inmunología, Hospital Universitario 12 de Octubre, Madrid, Spain; [b]Departamento de Bioquímica, Biología Molecular y Celular, Universidad de Zaragoza, Zaragoza, Spain; [c]Instituto de Investigación I+12, Madrid, Spain; and [d]Unidad de Inmunodeficiencias, Hospital Universitario 12 de Octubre, Madrid, Spain. E-mail: lallende.hdoc@salud.madrid.org.

This work was supported by grants from Fondo de Investigación Sanitaria (grant no. PI11/1591 to L.M.A.) and Ministerio de Economía y Competitividad, Spain (grant no. SAF2010-15341 to A.A.).

Disclosure of potential conflict of interest: L. Allende has received research support from Fondo de Investigaciones Sanitarias. A. Anel has received research support from the Ministerio de Economia y Competitividad. The rest of the authors declare that they have no relevant conflicts of interest.

REFERENCES

1. Renner ED, Puck JM, Holland SM, Schmitt M, Weiss M, Frosch M, et al. Autosomal recessive hyperimmunoglobulin E syndrome: a distinct disease entity. J Pediatr 2004;144:93-9.
2. Engelhardt KR, McGhee S, Winkler S, Sassi A, Woellner C, Lopez-Herrera G, et al. Large deletions and point mutations involving the dedicator of cytokinesis 8 (DOCK8) in the autosomal-recessive form of hyper-IgE syndrome. J Allergy Clin Immunol 2009;124:1289-302.
3. Zhang Q, Davis JC, Lamborn IT, Freeman AF, Jing H, Favreau AJ, et al. Combined immunodeficiency associated with DOCK8 mutations. N Engl J Med 2009;361:2046-55.
4. Randall KL, Chan SS, Ma CS, Fung I, Mei Y, Yabas M, et al. DOCK8 deficiency impairs CD8 T cell survival and function in humans and mice. J Exp Med 2011; 208:2305-20.
5. Brenchley JM, Karandikar NJ, Betts MR, Ambrozak DR, Hill BJ, Crotty LE, et al. Expression of CD57 defines replicative senescence and antigen-induced apoptotic death of $CD8^+$ T cells. Blood 2003;101:2711-20.
6. Appay V, van Lier RAW, Sallusto F, Roederer M. Phenotype and function of human T lymphocyte subsets: consensus and issues. Cytometry A 2008;73: 975-83.
7. Mizesko MC, Banerjee PP, Monaco-Shawver L, Mace EM, Bernal WE, Sawalle-Belohradsky J, et al. Defective actin accumulation impairs human natural killer cell function in patients with dedicator of cytokinesis 8 deficiency. J Allergy Clin Immunol 2013;131:840-8.
8. Ham H, Guerrier S, Kim J, Schoon RA, Anderson EL, Hamann MJ, et al. Dedicator of cytokinesis 8 interacts with talin and Wiskott-Aldrich syndrome protein to regulate NK cell cytotoxicity. J Immunol 2013;190:3661-9.
9. Bernardo I, Mancebo E, Aguiló I, Anel A, Allende LM, Guerra-Vales JM, et al. Phenotypic and functional evaluation of $CD3^+CD4^-CD8^-$ T cells in human CD8 immunodeficiency. Haematologica 2011;96:1195-203.

Available online March 14, 2014.
http://dx.doi.org/10.1016/j.jaci.2014.01.023

Flow cytometry diagnosis of dedicator of cytokinesis 8 (DOCK8) deficiency

To the Editor:

Biallelic mutations in the dedicator of cytokinesis 8 (*DOCK8*) gene cause autosomal-recessive hyper-IgE syndrome, a combined immunodeficiency characterized by sinopulmonary infections, skin and systemic viral infections, eczema, and food allergy. DOCK8 deficiency can lead to early death from infection and malignancy.[1,2] The disease is curable by hematopoietic cell transplantation (HCT).[3-5] Thus, it is important to ascertain the diagnosis of DOCK8 deficiency to institute early treatment.

The vast majority of DOCK8-deficient patients lack DOCK8 expression and many have deletions in the *DOCK8* gene.[1,2] Confirmation of the diagnosis has relied on immunoblotting of blood cell lysates and/or gene sequencing, techniques that are not routinely available. We present here a flow cytometry assay that could facilitate the diagnosis of DOCK8 deficiency, detection of carrier status, and investigation of lineage-specific DOCK8 expression following HCT.

The pedigrees of patients studied are shown in Fig E1 and their mutations in Table E1 (see Online Repository at www.jacionline.org). All studies were obtained after informed consent and approval of the Boston Children's Hospital Institutional Review Board. Intracellular staining for DOCK8 was performed on mononuclear cells from peripheral blood or bone marrow (BM) using the CytoFix/CytoPerm kit (BD Biosciences, San Jose, Calif), mouse monoclonal anti-DOCK8 (clone G-2, Santa Cruz Biotechnology, Dallas, Tex, raised against amino acids 119-277), mouse IgG_1 isotype control (Biolegend, San Diego, Calif), and fluorescein isothiocyanate–conjugated rat anti-mouse IgG_1 (Biolegend). Expression was calculated as the difference in mean fluorescence intensity (ΔMFI) between cells stained with anti-DOCK8 antibody and isotype control; the results were analyzed as a percentage of ΔMFI of healthy control assayed on the same day or in aggregate compared with the average of all healthy controls (see the Methods section in this article's Online Repository at www.jacionline.org).

Expression of DOCK8 could be detected by flow cytometry in subsets of normal peripheral blood and in $CD34^+$ BM cells (Fig 1, *A*). DOCK8 could not be detected by flow cytometry in T cells,

of CD57 and perforin expression on TEMRA $CD8^+$ T-cell subset. Columns show the expression of CD57 and perforin in naive, memory, and TEMRA $CD8^+$ T cells (mean ± SD of 2 independent experiments). **D,** Degranulation of $CD8^+$ T cells: CD107a surface expression in $CD8^+$ T cells after 6 hours of incubation in the presence (ratio 1:5) (E:T) or absence (ratio 1:0) of R69 target cells. Furthermore, PBMCs were stimulated with anti-CD3 mAb for 2 hours and degranulation was evaluated as indicated above. Cytotoxicity of $CD8^+$ T cells: the results represented the percentage of R69 cells positive for annexinV-FITC staining, as described by Bernardo et al.[9] Columns show the mean ± SD of 2 independent experiments. Statistical comparisons were performed with unpaired Student *t* tests, with significance defined as a $P < .05$. *FITC,* Fluorescein isothiocyanate.

CASE REPORT

The child of nonconsanguineous parents, he was a healthy, full-term infant. During his first year of life, he was diagnosed with bronchial asthma and atopic dermatitis. At 4 years, he had severe varicella and was later diagnosed with egg allergy. Since then, he has had several episodes of pneumonia, which led to bilateral bronchiectasis and mild-to-moderate obstructive lung disease. He has also had recurrent acute otitis media and mild *Molluscum contagiosum* around the penis. At 8 years, multiple and confluent flat warts appeared on his upper chest, shoulders, and groin. Intravenous immunoglobulin therapy was begun at age 9 years, which seemed to reduce the incidence of sinopulmonary infections. Currently aged 20 years, he also has a history of *Candida albicans* infection, recurrent angular cheilitis, chronic onychomycosis, and epidermodysplasia verruciformis. Immunologic assessment revealed moderate lymphopenia with decreases in $CD4^+$ (mean $\pm$ SD, 365 $\pm$ 118/uL since 7 years old), NK and switched memory B-cell levels. IgG and IgM were persistently low and IgA high. Immunization with *Streptococcus pneumoniae* and *Haemophilus influenzae* induced low levels of antibodies and no response, respectively (Table I).

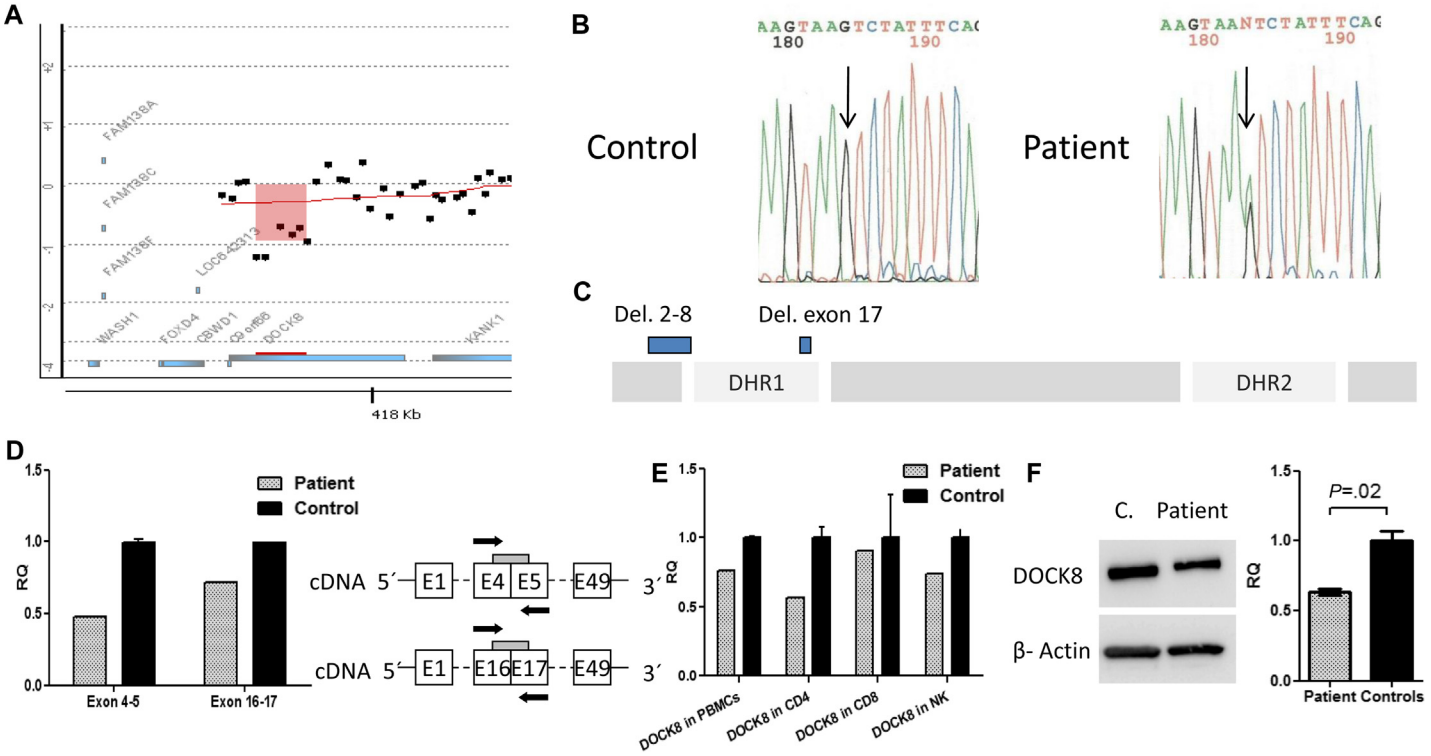

FIG E1. Molecular analyses in DOCK8 patient. **A,** CGH array showed copy number abnormalities consistent with heterozygous subtelomeric deletion of 9p *(red square)* spanning exons 2 to 8. **B,** DNA sequencing detected a heterozygous mutation (IVS17+5 G>A) in *DOCK8* gene of the patient. **C,** Schematic diagram of the DOCK8 protein and the location of patient's mutations. **D,** *DOCK8* transcript levels from the patient's PBMCs relative to healthy controls. Quantitative RT-PCR was used with exonic primers and a specific probe. When specific primers for the amplification of exons 4 and 5 (representative of exons 2-8 deletion allele in the patient) were used, controls were found to have 2 copies (RQ = 1) and the patient only 1 (RQ = 0.5) corresponding to the allele with the exon 17 deletion. When specific primers for the amplification of exons 16 and 17 (representative of exon 17 deletion allele in the patient) were used, controls also presented 2 copies (RQ = 1), while the patient presented more than 1 (RQ = 0.7), corresponding to the allele with exons 2 to 8 deletion (RQ = 0.5) and some normally spliced transcripts of the exon 17 allele (RQ = 0.2). GAPDH was used as the endogenous gene control. Data from 1 experiment using 3 healthy donors. **E,** Patient *DOCK8* gene expression levels in PBMCs, $CD4^+$, $CD8^+$, and NK cells are shown as relative expression with respect to that in normal cells, which is normalized to 1. Data from 1 experiment using 3 healthy donors. **F,** Partial DOCK8 expression in the patient's PBMCs. Western blot of DOCK8 and β-actin protein expression from a healthy control and the patient. Densitometric analysis of relative DOCK8 expression (DOCK8/β-actin) ± SD in 2 independent experiments is shown. Statistical analysis was performed with unpaired Student *t* tests, with significance defined as $P < .05$. Zhang et al[3] presented other case of partial DOCK8 expression among the 11 cases they described. *DHR1*, DOCK homology region 1; *DHR2*, DOCK homology region 2; *GAPDH*, glyceraldehyde-3-phosphate dehydrogenase.

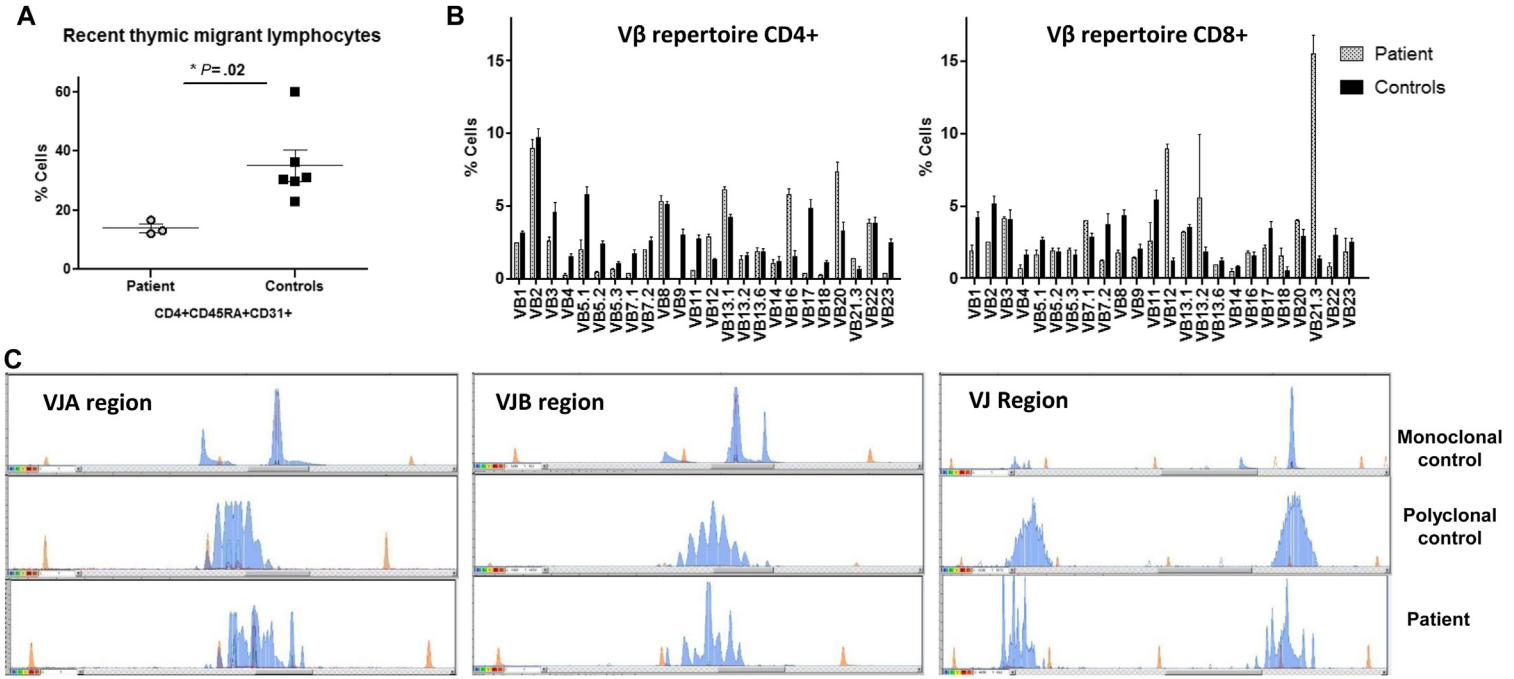

FIG E2. Thymic function. **A,** Recent thymic emigrant lymphocytes measured as $CD3^+CD4^+CD45RA^+CD31^+$ in the patient *(circles)* and in 6 age-matched controls *(squares)*. Statistical analysis was performed with unpaired Student *t* tests, with significance defined as $P < .05$. **B,** TCRVβ repertoire was determined by flow cytometry in gated $CD4^+$ and $CD8^+$ T cells from PBMCs of the patient (tested twice) and in 10 age-matched controls. **C,** Genomic *TCR VβJβ* rearrangements were amplified in the patient using 2 different primer sets (VBJB-A and VBJB-B) and compared with a normal (polyclonal) control and 2 tumor T-cell lines (monoclonal Jurkat or MOLT3) in the 240 to 280 bp range. Control T lymphocytes were polyclonal and thus showed a Gaussian fragment distribution (polyclonal control in the figure). T lymphoid tumors such as Jurkat or MOLT3 are monoclonal and thus yield a single major peak (monoclonal control in the figure). The results for the DOCK8 patient showed few peaks and did not follow a Gaussian distribution.

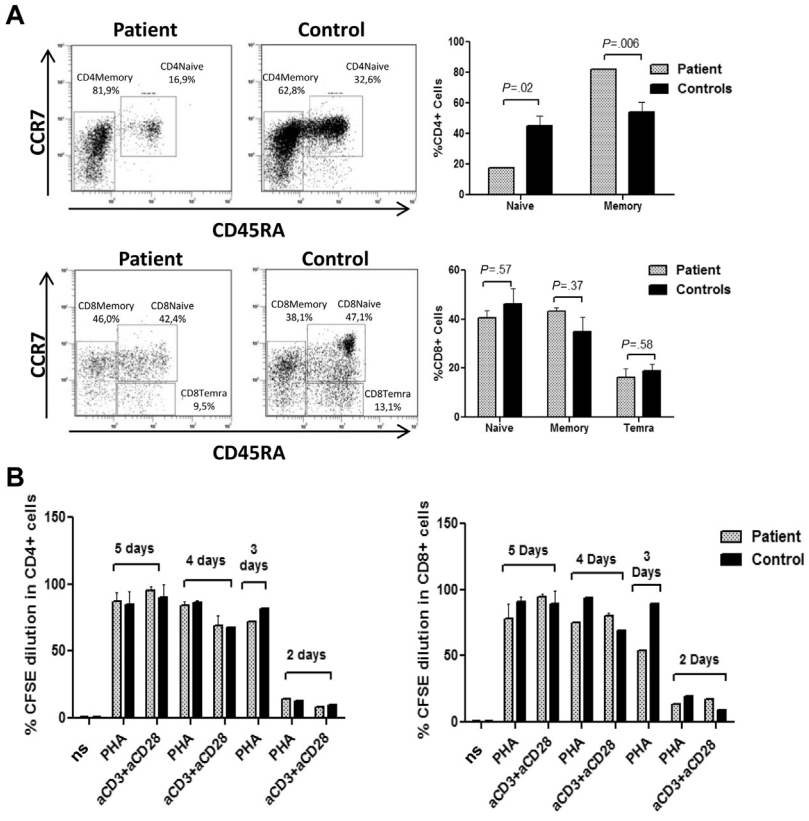

FIG E3. T-cell phenotype and function. **A,** Representative dot plots of $CD4^+$ and $CD8^+$ T-cell subsets (mean ± SD of 4 independent experiments). **B,** Lymphoproliferative capacity. PBMCs from the patient and controls were labeled with CFSE and were either nonstimulated *(ns)* or stimulated with PHA or anti-CD3 + anti-CD28 mAb. After 2, 3, 4, and 5 days of incubation, the percentage of CFSE dilution was depicted in gated $CD4^+$ and $CD8^+$ T cells (tested once for 2 and 3 days and twice for 4 and 5 days of stimulation). *CFSE*, Carboxyfluorescein succinimidyl ester.

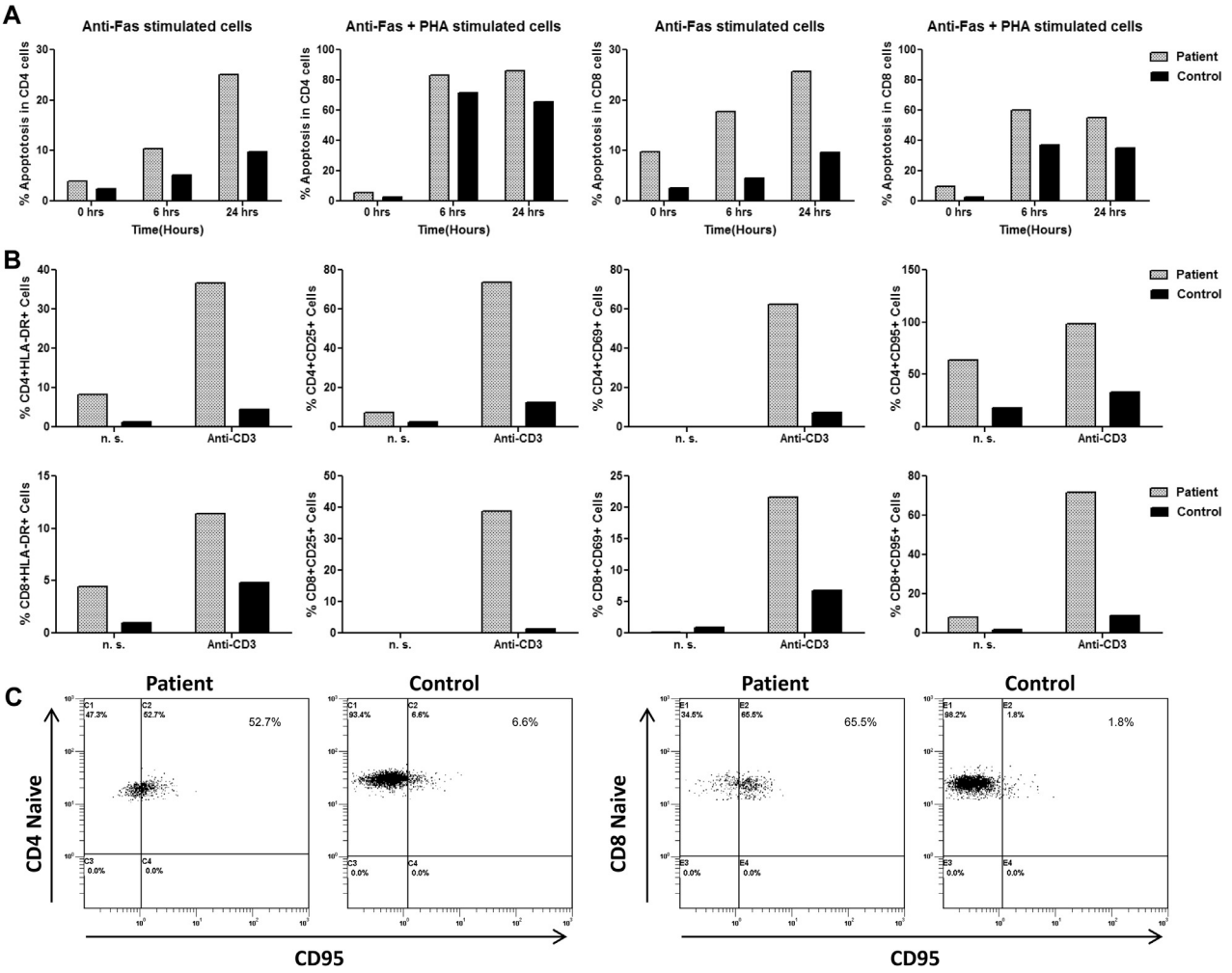

FIG E4. Higher expression of CD95 (Fas) correlated with higher sensitivity to Fas-induced apoptosis. **A,** PBMCs were either untreated (0 hour) or treated with agonist anti-Fas mAb alone or with anti-Fas mAb plus PHA, as indicated, for 6 or 24 hours. The percentage of apoptotic cells was measured by annexin V labeling in gated $CD4^+$ and $CD8^+$ T cells. **B,** PBMCs were not stimulated *(ns)* or stimulated with immobilized anti-CD3 mAb (clone UCHT1) (anti-CD3) for 24 hours. The expression of several activation surface markers, including CD95, was assessed in gated $CD4^+$ and $CD8^+$ T cells. **C,** Expression of CD95 in $CD4^+$ and $CD8^+$ naive T-cell subset. The results shown in this figure are from 1 of 2 experiments performed.

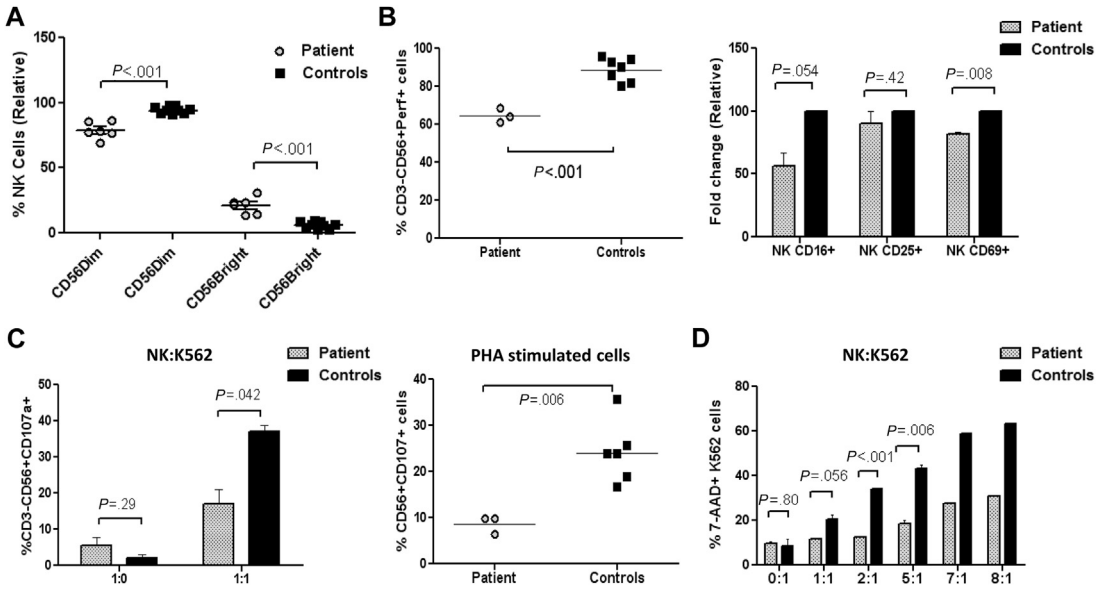

FIG E5. NK phenotype and functional assays. **A,** Relative differences between NK-cell subsets of the patient compared with healthy controls. **B,** Percentage of cells expressing perforin in NK cells *(left panel)*. NK cells were stimulated overnight with K562 cells (or without K562) and mean fluorescence intensity for CD16, CD25, and CD69 expression was calculated. The columns represent fold change in the patient relative to the control. Data are representative of 2 independent experiments *(right panel)*. **C,** Degranulation of NK cells: CD107a surface expression in NK cells after 6 hours of incubation in the presence (ratio 1:1) (E:T) or absence (ratio 1:0) of K562 target cells. Columns show the mean ± SD of 2 independent experiments. Furthermore, PBMCs were stimulated with PHA for 2 hours and degranulation was evaluated as indicated above. **D**, Cytotoxicity of NK cells: the results show the percentage of K562 cells incorporating 7-AAD (mean ± SD of 2 independent experiments, ratios 7:1 and 8:1 were only tested once). Statistical comparisons were performed with unpaired Student *t* tests, with significance defined as $P < .05$.

TABLE E1. Expression of NK markers in the DOCK8 patient and healthy controls

	Patient	Controls	*P* value
CD16	74.1 ± 2.5	93.4 ± 0.4	.008
CD25	1 ± 0.9	1.3 ± 0.8	NS
CD69	8.9 ± 4.5	14.8 ± 15.8	NS
DNAM-1	94.8 ± 1.1	96.0 ± 3.7	NS
CD11b	99.0 ± 0.4	99.8 ± 0.1	NS
NKp44	8.6 ± 3.4	2.4 ± 0.5	NS
NKG2D	96.7*	99.1 ± 0.21	—
NKp46	95.8 ± 2.6	97.2 ± 2.4	NS
NKp30	92.8 ± 4.2	95.7 ± 2.6	NS

Data are expressed as mean ± SD and represent the percentage of NK cells staining positive for each molecule. All tests were repeated twice unless indicated otherwise.
NS, Not significant.
*Tested only once.